

ORIGINAL ARTICLE

Equation Model for Predicting the Load Capacity of RC Hollow Beams

*Jen Hua Ling, Joseph Toh Sheng Ngu, Yong Tat Lim, Wen Kam Leong and How Teck Sia

Centre for Research of Innovation & Sustainable Development, School of Engineering and Technology, University of Technology Sarawak, 96000 Sibul, Sarawak, Malaysia

ABSTRACT - A reinforced concrete hollow beam has a void along its span. The void reduces the beam's weight while increasing its strength-to-weight ratio. It also reduces the moment of inertia and cross-sectional area, affecting the beam's load capacity. This effect is not considered by the existing beam theories, especially when the void is present in the tension zone. In this study, an equation model is derived to predict the load capacity of hollow beams. The reduced moment of inertia and cross-sectional area are considered while computing the moment and shear capacities, respectively. The model is then validated using experimental data from 11 specimens tested under a four-point load setup. In the specimens, PVC pipes of 25 mm to 75 mm in diameter were placed between 39 mm and 139 mm from the beam's soffit. From the validation analysis, the load capabilities are incorrectly predicted. The variation exceeds 10% of the experimental results, with a 36.1% average absolute error. Only four out of the eleven specimens' failure modes are correctly predicted. The model has a 95.4% chance predicting a 20% lower load capacity than the actual hollow beam. Thus, it could be used to design hollow beams. However, due to limited data, the hollow beam's shear strength is not verified. Thus, the model should not be used for hollow beams prone to

ARTICLE HISTORY

Received: 05 March 2023

Revised: 22 May 2023

Accepted: 23 June 2023

KEYWORDS

*Hollow beam,
PVC pipe,
Reinforced concrete,
Equation model,
Load capacity.*

INTRODUCTION

Concrete is an important construction material in Malaysia. One problem with concrete is the low strength-to-weight ratio [1]. It contributes to a weight penalty in structures with large open floor plans [2]. This is one of the greatest obstacles in designing members with a high strength-to-weight ratio [3]. This shortcoming has created the interest of researchers looking for solutions [4].

One way to reduce the concrete weight is by creating voids in RC beams. Lightweight materials are used as void formers, removing concrete from the sections. These materials include polyvinyl chloride pipes [5-18], polystyrene [19-26], polypropylene sheets [27], and plastic bottles [28];[29]. Most of these studies are experimental as the investigations were at the exploratory stage. Only a handful involved analytical derivations [10, 30].

The prevailing bending theory (Figure 1) assumes the concrete in the tension zone contributes nothing to a beam's bending resistance. This makes sense as the concrete would have cracked upon reaching its ultimate state. Nevertheless, this assumption has limitations. It disregards the effects of voids below the neutral axis. Based on the bending theory, removing the relevant concrete should not affect the beam's load capacity, but this is not the case in reality. The voids in beams were found to influence their load capacity to various extents [24];[25]. The beam's strength decreased as the size of the void increased [7];[10]. Therefore, in the context of RC hollow beams, applying the existing bending theory without any modification might overestimate the load capacity.

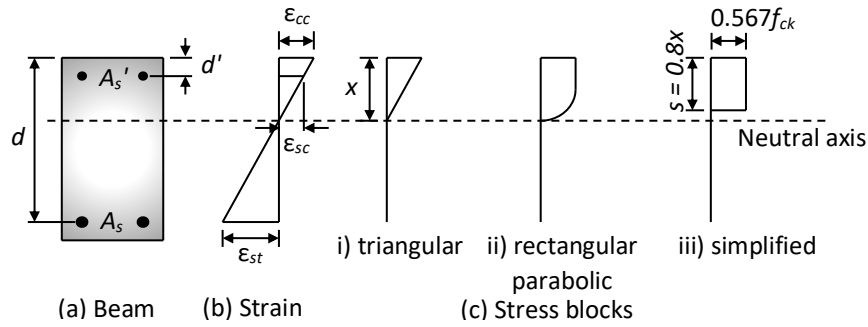


Figure 1. Stress block diagram of bending theory

In this study, an equation model is derived to predict the load capacities of RC hollow beams. The load capacity of a beam is thought to be governed by its moment of inertial and cross-sectional area. Thus, these properties are incorporated into the model. The purpose is to provide a simplified method for estimating the beam’s load capacity. The model is then validated using experimental data, and its reliability is evaluated.

EXPERIMENTAL DATA

Equations are derived based on the study by Ling et al. [18]. The relevant experimental data is used to validate the equations. The work comprised eleven (11) RC hollow beams, which were subjected to a four-point load test (Figure 2). The beam size was 150 mm by 300 mm by 1650 mm. Each beam was simply supported with a 1500 mm clear span. Two point loads were applied to the beam at 600 mm and 500 mm distances from the supports (Table 1).

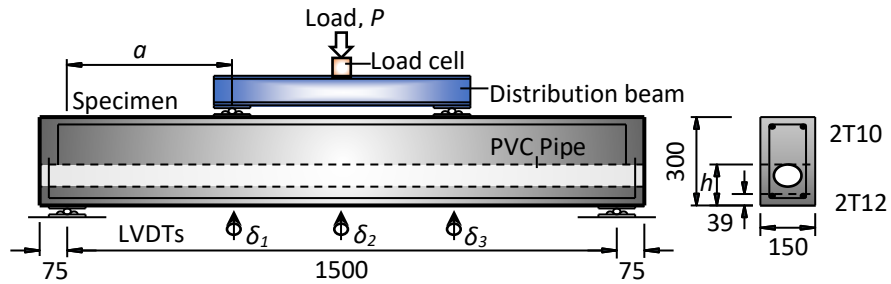


Figure 2. Test setup [18]

Table 1. Specimen details [18]

Specimen	PVC pipe		Point load	Shear reinforcement	a/d ratio
	Position, h_p (mm)	Diameter, d_p (mm)	Distance from support, a (mm)		
CB1	-	-	600	R8-150	2.3
CB2	-	-	500	R8-250	1.92
FB1	139	25	600	R8-150	2.3
FB2	64	25	600	R8-150	2.3
FB3	139	50	600	R8-150	2.3
FB4	89	50	600	R8-150	2.3
FB5	139	75	600	R8-150	2.3
FB6	114	75	600	R8-150	2.3
SB7	139	25	500	R8-250	1.92
SB8	139	50	500	R8-250	1.92
SB9	139	75	500	R8-250	1.92

*Effective depth of the beam, $d = 261$ mm

Each beam was reinforced with two bottom bars and two top bars with diameters of 12 mm and 10 mm, respectively. The bars' specified yield strength was 460 N/mm². The concrete cover was 25 mm. Thus, the effective depths to the bottom and top bars were 261 mm and 38 mm, respectively. Mild steel bars of 8 mm in diameter were used as shear links. The links had a specified yield strength of 250 N/mm² and were spaced at 150 mm and 250 mm (Table 1).

Polyvinyl chloride (PVC) pipes of 25 mm, 50 mm, and 75 mm in diameter formed the longitudinal voids in the beams. They were placed between 39 mm and 139 mm from the beam soffit (Figure 3). They were all in the tension zone of the hollow beams.

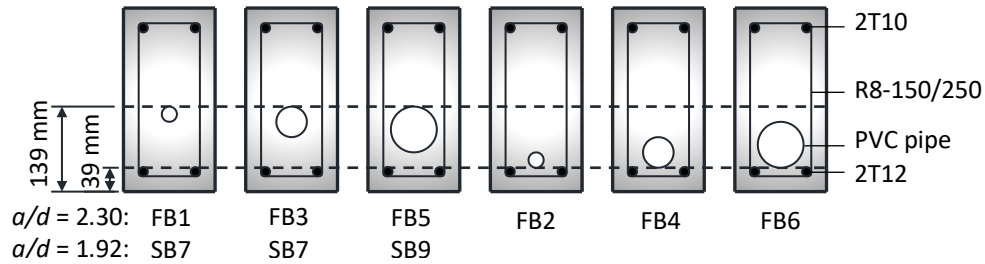


Figure 3. Position of PVC pipes by specimens.[18]

Table 2 displays the test results. The concrete strength ranged between 24.6 N/mm² and 27.8 N/mm², whereas the ultimate load varies from 100.4 kN to 163.1 kN. The failure modes included flexural, diagonal tension, and shear compression.

Table 2. Test results [18]

Specimen	Concrete strength, f_{cu} (N/mm ²)	Ultimate load, $P_{u,exp}$ (kN)	Failure mode
CB1	26.9	156.8	Flexural
CB2	25.9	163.1	Flexural
FB1	24.6	104.8	Flexural
FB2	25.8	133.1	Flexural
FB3	26.3	141.2	Diagonal tension
FB4	27.8	100.4	Diagonal tension
FB5	26.8	125.2	Shear compression
FB6	24.9	101.8	Diagonal tension
SB7	27.3	159.6	Shear compression
SB8	26.9	156.0	Shear compression
SB9	25.6	131.7	Shear compression

EQUATION DERIVATION

The derivation comprises the equations for predicting the specimens' load capacity, moment capacity, and shear capacity. The specimen's moment of inertia and cross-sectional area influence its moment and shear capacities. The moment and shear capacities subsequently govern the load capacity of the specimen.

Predicting load capacity

The specimen's load capacity, $P_{u,pre}$, is taken as the moment and shear capacities, whichever gives a smaller value [32] (Equation (1)).

$$P_{u,pre} = \min\{P_{u,m}, P_{u,v}\} \quad (1)$$

Where: $P_{u,m}$ = load capacity of the hollow beam due to the bending strength (kN), $P_{u,v}$ = load capacity of the hollow beam due to the shear strength (kN).

When $P_{u,m}$ is less than $P_{u,v}$, a beam fails in flexure, otherwise, shear failure is assumed [32]. The relevant strengths are given in Equation (2) and Equation (3). These equations are derived from the shear force and bending moment diagrams in Figure 4. These diagrams represent the response of a beam subjected to a four-point load test setup.

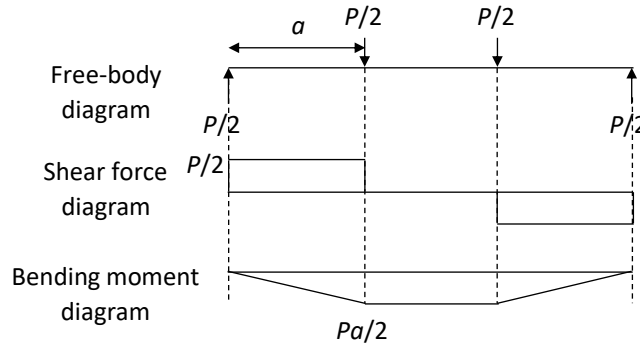


Figure 4. Response of a beam subjected to a four-point load test

$$P_{u,m} = \frac{2M_{u,pre}}{a} \quad (2)$$

$$P_{u,v} = 2V_{u,pre} \quad (3)$$

Where: $M_{u,pre}$ = predicted moment capacity of the hollow beam (kNm), a = distance between the point load and the support (m), $V_{u,pre}$ = predicted shear capacity of the hollow beam (kN).

Predicting moment capacity

Figure 5 shows the stress block diagram of a hollow beam subjected to bending. The moment capacity is predicted based on the following assumptions:

- The strain compatibility principle applies. Plane sections remain plane after bending. The steel strain is equivalent to the surrounding concrete strain.
- The forces in the plane are in equilibrium.
- The gross concrete section defines the beam's sectional properties.
- Bending occurred along the neutral axis. The concrete strain is proportional to the distance from the neutral axis. The maximum strain at the extreme concrete compression fibre is 0.0035.
- The beam is doubly reinforced due to the presence of compression reinforcement.
- The concrete has no tensile strength after cracking.
- A beam's moment of inertia determines its bending resistance. The void in a hollow beam reduces its moment of inertia and, subsequently, its moment capacity.
- A rectangular stress block of 0.8x height represents the parabolic stress profile at the ultimate state.
- The space occupied by the PVC pipe is considered void, which provides no flexural and shear strengths to the hollow beam.
- The tensile reinforcements have yielded at the ultimate state.

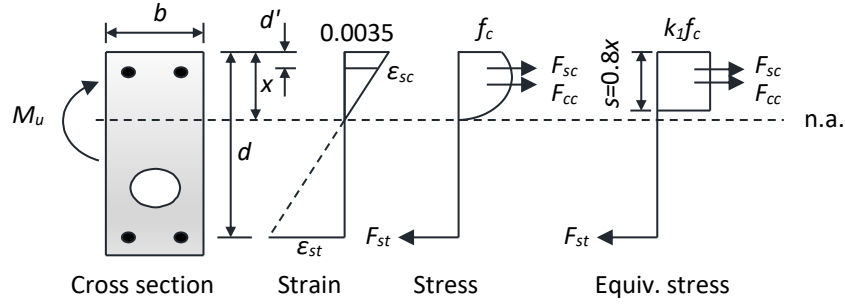


Figure 5. Stress and strain responses of a hollow beam subjected to pure bending

When the beam section is in equilibrium, the resultant force is equal to zero (Equation (4)).

$$F_{cc} + F_{sc} - F_{st} = 0 \quad (4)$$

Where: F_{cc} = compressive force of the concrete (kN), F_{sc} = compressive force of the top reinforcement (kN), F_{st} = tensile force of the bottom reinforcement (kN).

The force in concrete, F_{cc} , is given in Equation (5).

$$F_{cc} = 0.8x(b)(k_1 f_c) \quad (5)$$

Where: x = distance of the neutral axis from the beam's top fibre (mm), b = width of the beam's cross-section (mm), k_1 = a factor that correlates the compressive and flexural strengths of concrete, which is taken as 0.85 [33], f_c = compressive strength of concrete (N/mm²).

Equation (6) converts the cube strength, f_{cu} , into the cylinder strength, f_c . According to Kumari (2017) [34], f_{cu} is approximately 1.25 times f_c .

$$f_c = 0.8f_{cu} \quad (6)$$

The force in the compression reinforcement, F_{sc} , is determined using Equation (7). Its stress, σ_{sc} , is governed by the corresponding strain (Equation (8)), which is estimated through interpolation (Equation (9)). This is provided that the compression reinforcement has not yielded ($d'/x > 0.38$).

$$F_{sc} = \sigma_{sc} A_{sc} \quad (7)$$

$$\sigma_{sc} = \varepsilon_{sc} E_s \quad (8)$$

$$\varepsilon_{sc} = 0.0035 \frac{x - d'}{x} \quad (9)$$

Where: σ_{sc} = stress in compression reinforcement (N/mm²), A_{sc} = area of compression reinforcement (mm²), ε_{sc} = strain in compression reinforcement, E_s = modulus of elasticity of reinforcement, which is 205,000 N/mm² [35].

Substituting Equation (8) and Equation (9) into Equation (7), yields Equation (10)

$$F_{sc} = 0.0035 E_s A_{sc} \frac{x - d'}{x} \quad (10)$$

On the other hand, the force in the tensile reinforcement, F_{st} , is given in Equation (11).

$$F_{st} = A_{st}f_{st} \quad (11)$$

Substituting Equation (5), Equation (10), and Equation (11) into Equation (4), Equation (12) is obtained. The roots of Equation (12) would be the neutral axis, x , of the beam section (Equation (13)).

$$0.8bk_1f_c x^2 + (0.0035E_s A_{sc} - A_{st}f_{st})x - 0.0035E_s A_{sc}d' = 0 \quad (12)$$

$$x = \frac{(A_{st}f_{st} - 0.0035E_s A_{sc}) \pm \sqrt{(0.0035E_s A_{sc} - A_{st}f_{st})^2 + 0.0112bk_1f_c E_s A_{sc}d'}}{1.6bk_1f_c} \quad (13)$$

The moment capacity of the solid beam is calculated using Equation (14) (Figure 5).

$$M_b = F_{cc}z + F_{sc}(d - d') \quad (14)$$

Where: F_{cc} = force in the concrete (kN), F_{sc} = force in the compression reinforcement (kN), z = distance between the force of concrete and the force of tensile reinforcement (mm), d = effective depth of the tensile reinforcement (mm), d' = effective depth of the compression reinforcement (mm).

The lever arm, z , is expressed in Equation (15).

$$z = d - \frac{0.8x}{2} \quad (15)$$

The hollow beam's moment capacity is estimated using the effective moment of inertia (Equation (16)).

$$M_{u,pre} = \frac{I_e}{I_b} M_b \quad (16)$$

Where: I_e = effective moment of inertia of hollow beam (mm^4), I_b = moment of inertia of solid beam (mm^4), M_b = moment capacity of the solid beam (kNm).

The effective moment of inertia, I_e , is calculated as in Equation (17). The relevant moments of inertia, I_b and I_p , are derived against the neutral axis, x , using Equation (18) and Equation (19).

$$I_e = I_b - I_p \quad (17)$$

$$I_b = \frac{bh^3}{12} + A_b d_{yb}^2 \quad (18)$$

$$I_p = \frac{\pi d_p^2}{64} + A_p d_{yp}^2 \quad (19)$$

Where: I_b = moment of inertia of solid beam (mm^4), I_p = moment of inertia of void in the beam (mm^4), I_b = moment of inertia of solid beam (mm^4), I_p = moment of inertia of void in the beam (mm^4), d_p = diameter of PVC pipe (mm), A_p = concrete area occupied by the PVC pipe (mm), d_{yp} = cross-sectional area of PVC pipe (mm^2).

Predicting shear capacity

A hollow beam's shear resistance, V_u , is due to the concrete, V_c , and shear reinforcement, V_s (Equation (20)) [33].

$$V_u = V_c + V_s \quad (20)$$

Where: V_c = shear strength provided by concrete (kN), V_s = shear strength provided by shear reinforcement (kN).

The void in a hollow beam reduces its cross-sectional area, affecting the shear strength. The effective cross-sectional area is considered when calculating the shear resistance, V_c (Equation (21)).

$$V_c = \frac{A_e}{A_b} V_{R,c} \quad (21)$$

Where: A_e = effective cross-sectional area of the hollow beam, mm^2 , A_b = cross-sectional area of the solid beam, mm^2 , $V_{R,c}$ = shear resistance of the solid beam without shear reinforcement (kN).

Equation (22) gives the shear resistance of a solid beam without shear reinforcement, $V_{R,c}$ [35].

$$V_{R,c} = \left[C_{R,c} k (100 \rho_1 f_c)^{\frac{1}{3}} \right] b d \quad (22)$$

Where: $C_{R,c} = 0.18$ (disregard the partial factor of safety for concrete), $k = 1 + \sqrt{\frac{200}{d}}$, $\rho_1 = \frac{A_{st}}{bd} \leq 0.02$, f_c = compressive strength of concrete (N/mm^2), b = width of the beam (mm), d = effective depth of the tensile reinforcement (mm), A_{st} = the area of tensile reinforcement, mm^2

Equation (23) expresses the shear resistance provided by shear reinforcement, V_s [35].

$$V_s = \frac{A_{sw}}{s} z_{sw} f_{yw} \cot \theta \quad (23)$$

Where: A_{sw} = the cross-sectional area of the shear reinforcement (mm^2), s = the spacing of the shear reinforcement (mm), z_{sw} = the inner lever arm (taken as 0.9 times the effective depth, d), f_{yw} = the specified yield strength of the shear reinforcement (N/mm^2), $\theta = 45^\circ$ (assumed value for critical shear load).

When the load is placed within $0.5d$ to $2d$ of the supports (Figure 6), the shear load, V_a , in a beam may be reduced by a factor β (Equation (24)) [35]. This only applies to specimens CB2, SB7, SB8, and SB9 with a equals to $1.92d$. For the other specimens, the load is not within the range of $0.5d$ to $2d$ from the supports.

$$V_r = V_a \times \beta \quad (24)$$

Where: V_a = applied shear load (kN), β = reduction factor (when $a = 1.92d$, $\beta = a/2d$; otherwise $\beta = 1.0$), a = distance between the point load and the support (mm), d = effective depth of the tensile reinforcement (mm).

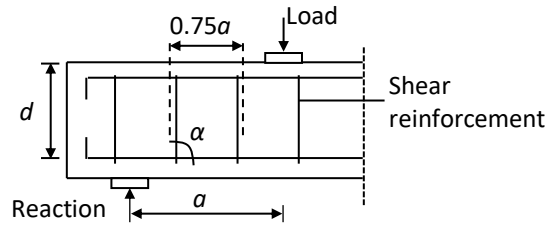


Figure 6. Shear reinforcement within the central $0.75a$

This effective shear load, V_r , is resisted by the shear reinforcement within the central $0.75a$ [35]. The shear resistance is given in Equation (25).

$$V_r = nA_{sw}f_{yw} \sin \alpha \quad (25)$$

Where: n = numbers of shear reinforcement within the central $0.75a$ ($n = 3$ for R8-150, $n = 2$ for R8-250), A_{sw} = the cross-sectional area of one unit of shear reinforcement (mm^2), f_{yw} = the specified yield strength of the shear reinforcement (N/mm^2), α = angle of inclined shear reinforcement (90° for vertical links).

Combining Equation (24) and Equation (25) yields Equation (26). The equation represents the shear resistance of the specimen under a four-point load setup.

$$V_a = \frac{nA_{sw}f_{yw} \sin \alpha}{\beta} \quad (26)$$

The predicted shear capacity of the hollow beam, $V_{u,pre}$, would be the larger value of the two shear resistances.

$$V_{u,pre} = \max\{V_u, V_a\} \quad (27)$$

EQUATION VALIDATION

Table 3 shows the predicted moment capacities of the specimens based on the equation model. The neutral axis, x , is between 41.6 mm and 44 mm (Table 3). This means that the void is always in the tension region of the hollow beam. The concrete carries more compressive force than the compression bars ($F_{cc} > F_{sc}$). The model predicted a lower moment capacity for a hollow beam than for a solid beam. M_{pre} is always smaller than M_b . M_{pre} considers the effects of the void in the beam, whereas M_b disregards it.

Table 3. Estimating the moment capacities of hollow beams

	f_c (N/mm ²)	x (mm)	F_{cc} (kN)	z (mm)	F_{sc} (kN)	M_b (kNm)	d_{yb} (mm)	I_b (x10 ⁶ mm ⁴)	y_p (mm)	d_{yp} (mm)	I_p (x10 ⁶ mm ⁴)	I_e (x10 ⁶ mm ⁴)	M_{pre} (kNm)
Eq	(6)	(13)	(5)	(15)	(11)	(14)		(18)			(19)	(17)	(16)
CB1	21.5	42.2	92.5	244.1	11.2	25.1	107.8	860.4	0	0	0	860.4	25.1
CB2	20.7	43.0	90.8	243.8	13.1	25.1	107.0	852.7	0	0	0	852.7	25.1
FB1	19.7	44.0	88.4	243.4	15.4	24.9	106.0	843.1	173.5	129.5	8.2	834.9	24.7
FB2	20.6	43.1	90.6	243.8	13.3	25.1	106.9	851.7	248.5	205.4	20.7	831.0	24.4
FB3	21.0	42.7	91.5	243.9	12.4	25.1	107.3	855.6	186.0	143.3	40.3	815.3	23.9
FB4	22.2	41.6	94.2	244.4	9.7	25.2	108.4	866.3	236.0	194.4	74.2	792.1	23.0
FB5	21.4	42.3	92.3	244.1	11.5	25.1	107.7	859.5	198.5	156.2	107.8	751.7	21.9
FB6	19.9	43.8	88.9	243.5	14.9	25.0	106.2	845.0	223.5	179.7	142.7	702.4	20.8
SB7	21.8	42.0	93.4	244.2	10.7	25.2	108.0	862.4	173.5	131.5	8.5	853.9	25.0
SB8	21.5	42.2	92.5	244.1	11.2	25.1	107.8	860.4	186.0	143.8	40.6	819.8	23.9
SB9	20.5	43.2	90.3	243.7	13.6	25.0	106.8	850.8	198.5	155.3	106.6	744.2	21.9

*Note: $A_{st} = 226 \text{ mm}^2$ (2T12), $f_{st} = 460 \text{ N/mm}^2$, $E_s = 205 \text{ GPa}$, $A_{sc} = 157 \text{ mm}^2$ (2T10), $b = 150 \text{ mm}$, $k_1 = 0.85$, $d' = 38 \text{ mm}$, $d = 261 \text{ mm}$, $h = 300 \text{ mm}$, $y_b = 150 \text{ mm}$, h_p and d_p refer to Table 1, f_{cu} refer to Table 2.

Table 4 presents the predicted shear capacities of the specimens. The void in the hollow beam affects the shear strength of concrete. V_c is always less than $V_{R,c}$ due to the smaller effective cross-sectional area. The model disregards the effects of the void on the shear resistance given by the shear reinforcement, i.e., V_s and V_a .

Table 4. Estimating the shear capacities of hollow beams

Specimen	A_e (mm ²)	$V_{R,c}$ (kN)	V_c (kN)	s (mm)	V_s (kN)	V_u (kN)	n	β	V_a (kN)	$V_{u,pre}$ (kN)
Equation		(22)	(21)		(23)	(20)			(26)	(27)
CB1	45,000	30.6	30.6	150	39.5	70.1	3	1.000	75.8	75.8
CB2	45,000	30.2	30.2	250	23.7	53.9	2	0.958	52.7	53.9
FB1	44,509	29.7	29.4	150	39.5	68.9	3	1.000	75.8	75.8
FB2	44,509	30.2	29.8	150	39.5	69.4	3	1.000	75.8	75.8
FB3	43,037	30.3	29.0	150	39.5	68.6	3	1.000	75.8	75.8
FB4	43,037	30.9	29.6	150	39.5	69.1	3	1.000	75.8	75.8
FB5	40,582	30.5	27.5	150	39.5	67.1	3	1.000	75.8	75.8
FB6	40,582	29.8	26.9	150	39.5	66.4	3	1.000	75.8	75.8
SB7	44,509	30.7	30.4	250	23.7	54.1	2	0.958	52.7	54.1
SB8	43,037	30.6	29.3	250	23.7	53.0	2	0.958	52.7	53.0
SB9	40,582	30.1	27.1	250	23.7	50.9	2	0.958	52.7	52.7

*Note: $A_b = bh = 45,000 \text{ mm}^2$, $A_e = A_b - \pi d_p^2/4$, $b = 150 \text{ mm}$, $h = 300 \text{ mm}$, $C_{R,d} = 0.18$, $k = 1.875$, $\rho_1 = 0.00577$, $A_{sw} = 101 \text{ mm}^2$ (R8 shear link), $f_{yw} = 250 \text{ N/mm}^2$, $d = 261 \text{ mm}$, $z_{sw} = 0.9d = 234.9 \text{ mm}$, f_c refer to Table 3, a and d_p refer to Table 1.

Table 5 exhibits the load capacities of the specimens predicted by the equation model. The predicted moment capacity, $P_{u,m}$, is always less than the predicted shear capacity, $P_{u,v}$, and so governs the specimens'

load capacity, $P_{u,pre}$. For that reason, all the specimens are predicted to fail in flexure (Table 6). The predicted results are then compared with the experimental results for validation purposes.

Table 5. Validation of the predicted load capacity

Specimen	$P_{u,m}$ (kN)	$P_{u,v}$ (kN)	$P_{u,pre}$ (kN)	$P_{u,exp}$ (kN)	R_r	Remarks *	$\frac{P_{u,pre} - P_{u,exp}}{P_{u,exp}}$
Ref.	Eq. (2)	Eq. (3)	Eq. (1)	Table 2	Eq. (28)		
CB1	83.6	151.6	83.6	156.8	0.53	X	0.47
CB2	100.2	107.8	100.2	163.1	0.61	X	0.39
FB1	82.3	151.6	82.3	104.8	0.79	X	0.21
FB2	81.5	151.6	81.5	133.1	0.61	X	0.39
FB3	79.6	151.6	79.6	141.2	0.56	X	0.44
FB4	76.8	151.6	76.8	100.4	0.76	X	0.24
FB5	73.2	151.6	73.2	125.2	0.58	X	0.42
FB6	69.2	151.6	69.2	101.8	0.68	X	0.32
SB7	99.8	108.2	99.8	159.6	0.63	X	0.37
SB8	95.6	106.0	95.6	156.0	0.61	X	0.39
SB9	87.6	105.4	87.6	131.7	0.67	X	0.33
				Mean	0.64	Sum	4.00
				SD	0.08	AAE (Eq. 29)	36.1

*Note: \checkmark when $0.9 \leq R_r \leq 1.1$, X when $R_r < 0.9$ or $R_r > 1.1$.

Table 6. Validation of the predicted failure mode

Specimen	Predicted failure mode	Actual failure mode	Remarks * ²
CB1	F	F	\checkmark
CB2	F	F	\checkmark
FB1	F	F	\checkmark
FB2	F	F	\checkmark
FB3	F	DT	X
FB4	F	DT	X
FB5	F	S	X
FB6	F	DT	X
SB7	F	S	X
SB8	F	S	X
SB9	F	S	X

*Note: ¹F – Flexural failure, DT – Diagonal tension failure, S – Shear failure; ² \checkmark when predicted failure = experimental failure, X when predicted failure \neq experimental failure.

The reliability of the equation model can be tested using a ratio, R_r (Equation (28)). When a majority of the specimens ($\geq 80\%$) have the predicted load within 10% variation from the experimental results ($0.9 \leq R_r \leq 1.1$), the equation model is considered reliable [22].

$$R_r = \frac{P_{pre}}{P_{exp}} \quad (28)$$

Where: P_{pre} = Predicted load capacity of the hollow beam (kN), P_{exp} = Experimental load capacity of the hollow beam (kN)

The accuracy of the equation model can be quantified using an Average Absolute Error (AAE) (Equation (29)) [36, 37]. The larger the value, the greater the error predicted by the model.

$$AAE = \frac{\sum_{i=1}^N \left| \frac{P_{u,pre,i} - P_{u,exp,i}}{P_{u,exp,i}} \right|}{N} \times 100 \quad (29)$$

Where: N = total number of specimens, $P_{u,pre}$ = predicted load capacity (kN), $P_{u,exp}$ = experimental load capacity (kN).

The equation model incorrectly predicts the hollow beams' load capacities. The average absolute error, AAE, is 36.1%, which is quite significant. The model is not reliable, since none of the predicted loads met the 10% variation limit. Furthermore, only four out of eleven failure modes are correctly forecasted. The model anticipates the load capacity conservatively. The mean R_r is 0.64, which is 36% lower than the experimental results. The standard deviation is 0.08. This suggests that R_r between 0.48 and 0.8 has a 95.4% confidence level (i.e., the mean ± 2 times the standard deviation). In other words, the predicted load capacity has a 95.4% chance of being 20% lower than the actual load capacity.

The equation model predicts a lower load capacity due to several conservative assumptions:

- The specified yield stress of the reinforcements is used in the model. The actual yield stress is usually higher, resulting in a stronger beam.
- At the beam's ultimate state, the tensile reinforcement would have yielded. However, it has not deformed sufficiently to achieve the ultimate stress. The model does not account for the benefits of post-yielding stress. The bending strength would have been overestimated if the ultimate stress had been used. It would have been underestimated if the yield stress had been adopted.
- The flexural and shear strengths provided by the PVC pipes in the hollow beams are ignored by the model. If they are considered, the load capacity would be slightly larger.

It is worth noting that the equation model's derivation procedure is not entirely analytical. The reductions of the moment and shear capacities are considered to be proportional to the reduction of the moment of inertia and cross-sectional area, respectively. This may not be the case in reality. In addition, The predicted load capacity is computed without incorporating the partial factor of safety for materials. If those are applied in the equation model, the load capacity would be lower.

Because the model disregards the strength of PVC pipes, it can be applied to various types of hollow beams. Despite the longitudinal void, the void can be any shape that is closely spaced across the beam's span. The load capacity anticipated by the model would be similar. Polystyrene and other lightweight materials may be used to form the void in the beam.

Due to the limited data, the validation results are potentially biased. The predicted shear capacity cannot be reasonably validated because none of the specimens is anticipated to fail in shear. Although the fundamental equations (i.e., Equation (22), Equation (23), and Equation (25)) are taken from Eurocode 2 [35], their applicability in hollow beams should have been verified in this study. This cannot be done using the present data set. Thus, the application of the model to hollow beams prone to shear failure is still questionable.

If the PVC pipe is put within the compressive zone, the model would be inapplicable. The void would have disrupted the compressive stress block, decreasing the hollow beam's load capacity [10]. Also, the

specimens validating the equation model have a PVC pipe diameter not exceeding 75 mm, which is half the beam width ($d_p \leq 0.5b$). It is unsure if the model is also applicable for pipe sizes larger than that.

The model anticipates the hollow beams either failing in flexure or shear. It does not forecast diagonal tension failure. Also, when the void is too close to the reinforcements, the bond with the concrete may be compromised [23]. The void should avoid sharp corners to reduce its detrimental effect on the load capacity [8, 38]. The model does not account for these situations. The model may need to be further refined in future studies.

This model adopts the simplified approach of the existing beam theory (Figure 1) and disregards the post-yield response of the reinforcements in hollow beams. This inevitably inherits the shortcomings of the existing beam theory, in which the predicted load capacity is much lower than the actual load capacity. In reality, the non-linear properties of materials after yielding influence a beam's load capacity. To deal with the complexity of the stress-strain configuration within the beam, future studies may employ numerical analysis based on finite element models.

CONCLUSION

In this study, an equation model is derived to predict the load capacity of reinforced concrete hollow beams. In the model, the effects of the reduced moment of inertia and cross-sectional area on the load capacity are considered.

The model is validated with experimental results. The model predicts the load capacity inaccurately, with an average absolute error of 36.1%. None of the predicted results are within a 10% variation of the experimental results. A majority of the failure modes (7 out of 11 specimens) are wrongly predicted. Nonetheless, the model has a 95.4% chance of predicting a 20% lower load capacity than that of the actual hollow beam. This is provided that (a) the PVC pipe is not located in the compressive zone of the beam's section, (b) the size of the PVC pipe is not larger than half the beam's width, and (c) the PVC pipe does not impair the bond between the reinforcements and concrete.

The validation does not cover the shear capacity due to limited data. The equation model may not apply to hollow beams prone to shear failure. It should not be used until it is thoroughly proven.

ACKNOWLEDGEMENT

This study was supported by the Research Grants of the University of Technology Sarawak, UCTS/RESEARCH/2/2018/02.

REFERENCES

- [1] H. S. Dweik, M. M. Ziara, and M. S. Hadidoun, "Enhancing concrete strength and thermal insulation using thermoset plastic waste," *International Journal of Polymeric Materials and Polymeric Biomaterials*, vol. 57, no. 7, pp. 635-656, 2008, doi: 10.1080/00914030701551089.
- [2] Z. M. Jaini, H. B. Koh, S. N. Mokhtatar, I. Mat, H. Hazmi, and N. H. Hashim, "Structural behaviour of short-span reinforced concrete beams with foamed concrete infill," *ARPN Journal of Engineering and Applied Sciences*, vol. 11, no. 16, pp. 9820-9824, 2016.
- [3] N. S. Ramli, and N. Abd Rahman, "Strength of modified foam concrete filled hollow section using fly ash as sand replacement added polypropylene fibre," *Recent Trends in Civil Engineering and Built Environment*, vol. 3, no. 1, pp. 1022-1028, 2022, doi: 10.1088/1757-899X/1200/1/012016.
- [4] N. Mohamad, W. I. Goh, A. A. A. Samad, A. Lockman, and A. Alalwani, "Structural behaviour of beam with HDPE plastic balls subjected to flexural load," *Materials Science Forum*, vol. 889, pp. 270-274, 2017, doi: 10.4028/www.scientific.net/MSF.889.270
- [5] K. Sherin, and S. Abhirami, "Analytical study on geopolymer concrete beam with hollow space below neutral axis," *International Journal of Advance Engineering and Research Development*, vol. 5, no. 5, pp. 332-342, 2018.
- [6] J. Joy, and R. Rajeev, "Effect of reinforced concrete beam with hollow neutral axis," *International Journal for Scientific Research & Development*, vol. 2, no. 10, pp. 341-348, 2014.
- [7] L. Ragavi, "Behaviour of reinforced concrete hollow beams under monotonic loading," *World Journal of Technology, Engineering and Research*, vol. 2, no. 1, pp. 127-136, 2017.

- [8] B. P. Bhattarai, and N. Bhattarai, "Experimental study on flexural behavior of reinforced solid and hollow concrete beams," *International Journal of Engineering Research and Advanced Technology*, vol. 3, no. 11, pp. 1-8, 2017.
- [9] S. Soji, and P. Anima, "Experimental and analytical investigation on partial replacement of concrete in the tension zone," *International Journal of Engineering Research and General Science*, vol. 4, no. 4, pp. 23-32, 2016.
- [10] A. Murugesan, and A. Narayanan, "Influence of a longitudinal circular hole on flexural strength of reinforced concrete beams," *Practice Periodical on Structural Design and Construction*, vol. 22, no. 2, pp. 04016021-1 - 04016021-10, 2016, doi: 10.1061/(ASCE)SC.1943-5576.0000307
- [11] N. P. Dhinesh, and V. S. Satheesh, "Flexural behaviour of hollow square beam," *International Journal of Scientific Engineering and Applied Science*, vol. 3, no. 3, pp. 236-242, 2017.
- [12] A. M. Kuriakose, M. M. Paul, "Behaviour of beams with low grade concrete or hollow neutral axis zone," *International Journal of Civil Engineering and Technology*, vol. 6, no. 10, pp. 185-190, 2015.
- [13] N. Parthiban, and M. Neelamegam, "Flexural behavior of reinforced concrete beam with hollow core in shear section," *International Research Journal of Engineering and Technology*, vol. 4, no. 4, pp. 2263-2274, 2017.
- [14] N. Varghese, and A. Joy, "Flexural behaviour of reinforced concrete beam with hollow core at various depth," *International Journal of Science and Research*, vol. 5, no. 5, pp. 741-756, 2016.
- [15] G. Balaji, and R. Vetturayasudharsanan, "Experimental investigation on flexural behaviour of RC hollow beams," *Materialstoday: Proceeding*, vol. 21, no. 1, pp. 351-356, 2020, doi: 10.1016/j.matpr.2019.05.461.
- [16] H. N. G. Mohammed Al-Maliki, "Experimental behavior of hollow non-prismatic reinforced concrete beams retrofitted with CFRP sheets," *Journal of Engineering and Development*, vol. 17, no. 5, pp. 224-237, 2013.
- [17] T. S. S. Al-Gasham, "Reinforced concrete moderate deep beams with embedded PVC pipes," *Wasit Journal of Engineering Science*, vol. 3, no. 1, pp. 19-28, 2015.
- [18] J. H. Ling, J. T. S. Ngu, Y. T. Lim, W. K. Leong, and H. T. Sia, "Experimental study of RC hollow beams with embedded PVC pipes," *Journal of Advanced Civil and Environmental Engineering*, vol. 5, no. 1, pp. 11-23, 2022, doi: 10.30659/jacee.5.1.11-23.
- [19] A. J. H. Alshimmeri, and H. N. G. Al-Maliki, "Structural behavior of reinforced concrete hollow beams under partial uniformly distributed load," *Journal of Engineering*, vol. 20, no. 7, pp. 130-145, 2014.
- [20] S. Manikandan, S. Dharmar, and S. Robertravi, "Experimental study on flexural behaviour of reinforced concrete hollow core sandwich beam," *International Journal of Advance Research in Science and Engineering*, vol. 4, no. 1, pp. 937-946, 2015.
- [21] D. T. L. Tan, and J. H. Ling, "Flexural behaviour of reinforced concrete beam embedded with different alignment of polystyrene," *Borneo Journal of Sciences and Technology*, vol. 2, no. 1, pp. 13-18, 2020, doi: 10.35370/bjost.2020.2.1-04
- [22] J. H. Ling, L. L. Chan, W. K. Leong, and H. T. Sia, "The development of finite element model to investigate the structural performance of reinforced concrete hollow beams," *Journal of the Civil Engineering Forum*, vol. 6, no. 2, pp. 171-182, 2020, doi: 10.22146/jcef.53301
- [23] J. W. Lau, J. H. Ling, and Y. T. Lim, "Feasibility study of reinforced concrete beam with embedded polystyrene spheres under incremental flexural load," *Borneo Journal of Social Science & Technology*, vol. 2, no. 2, pp. 11-26, 2020, doi: 10.3570/bjost.2020.2.2-04.
- [24] Y. T. Lim, J. H. Ling, J. W. Lau, and T. T. L. Danson, "Performance of reinforced concrete beam with polystyrene blocks at various regions," *Journal of Science and Applied Engineering*, vol. 3, no. 2, pp. 62-71, 2021, doi: 10.31328/jsae.v3i2.1655
- [25] Y. T. Lim, J. H. Ling, J. W. Lau, and A. Y. M. Yik, "Experimental study on the flexural behavior of reinforced polystyrene blocks in concrete beams," *Journal of the Civil Engineering Forum*, vol. 7, no. 2, pp. 197-208, 2021, doi: 10.22146/jcef.62346.
- [26] A. Varghese, and B. M. Joseph, "Experimental and numerical studies on reinforced concrete hollowcore sandwich beams," *International Journal of Innovative Research in Science, Engineering and Technology*, vol. 5, no. 8, pp. 14730-14737, 2016.
- [27] U. N. Kumbhar, and H. S. Jadhav, "Flexural behaviour of reinforced concrete hollow beam with polypropylene plastic sheet infill," *International Research Journal of Engineering and Technology*, vol. 5, no. 5, pp. 1517, 2018.
- [28] I. Mathew, and S. M. Varghese, "Experimental study on partial replacement of concrete in and below neutral axis of beam," *International Journal of Innovative Research in Technology*, vol. 3, vol. 4, pp. 188-192, 2016.
- [29] S. Sariman, and A.R. Nurdin, "Flexural behavior of T shaped reinforced concrete hollow beam with plastic bottle waste," *International Journal of Civil Engineering and Technology*, vol. 9, no. 4, pp. 534-543, 2018.
- [30] Y. M. Al-Smadi, N. Al-Huthaifi, and A. A. Alkhawaldeh, "The effect of longitudinal hole shape and size on the flexural behavior of RC beams," *Results in Engineering*, vol. 16, 100607, 2022, doi:

- 10.1016/j.rineng.2022.100607.
- [31] C. Bailey, T. Bull, and A. Lawrence, "The bending of beams and the second moment of area," *The Plymouth Student Scientist*, vol. 6, no. 2, pp. 328–339, 2013.
 - [32] J. H. Ling, H. S. Tang, W. K. Leong, and H. T. Sia, "Behaviour of reinforced concrete beams with circular transverse openings under static loads," *Journal of Science and Applied Engineering*, vol. 3, no. 1, pp. 1-16, 2020, doi: 10.31328/jsae.v3i1.1288
 - [33] ACI 318-19 Building Code Requirements for Structural Concrete, *American Concrete Institute*, 2019.
 - [34] R. Kumari, "Review paper based on the relation between the strength of concrete cubes and cylinders," *International Journal of Engineering Research and Applications*, vol. 5, no. 8, pp. 52-54, 2015.
 - [35] British Standards, Eurocode 2: Design of concrete structures - Part 1-1: General rules and rules for buildings, BS-EN 1992-1-1:2004, 2004.
 - [36] A. M. Woldemariam, W. O. Oyawa, and T. Nyomboi, "The behavior of concrete-filled single and double-skin uPVC tubular columns under axial compression loads," *The Open Construction and Building Technology Journal*, vol. 13, pp. 164-177, 2019, doi: 10.2174/1874836801913010164.
 - [37] A. M. Woldemariam, W. O. Oyawa, and T. Nyomboi, "Structural performance of uPVC confined concrete equivalent cylinders under axial compression loads," *Buildings*, vol. 9, no. 4, 82, 2019, doi: 10.3390/buildings9040082.
 - [38] Y. T. Lim, and J. H. Ling, Incorporating lightweight materials in reinforced concrete beams and slabs – A review, *Borneo Journal of Sciences and Technology*, vol. 1, no. 2, pp. 16-26, 2019, doi: 10.35370/bjost.2019.1.2-03.